Journal of Solid Mechanics Vol. 12, No. 2 (2020) pp. 385-400
DOI: 10.22034/jsm.2019.1869981.1450

Free Vibration Analysis of Bidirectional Functionally Graded Conical/Cylindrical Shells and Annular Plates on Nonlinear Elastic Foundations, Based on a Unified Differential Transform Analytical Formulation

M. Molla Alipour [1], M. Shariyat [2], M. Shaban [3, *]

[1] *Department of Mechanical Engineering, University of Mazandaran, Babolsar , Iran*
[2] *Faculty of Mechanical Engineering, K.N. Toosi University of Technology, Tehran, Iran*
[3] *Mechanical Engineering Department, Bu-Ali Sina University, Hamadan, Iran*

Received 7 March 2020; accepted 3 May 2020

ABSTRACT

In the present research, a unified formulation for free vibration analysis of the bidirectional functionally graded conical and cylindrical shells and annular plates on elastic foundations is developed. To cover more individual cases and optimally tailored material properties, the material properties are assumed to vary in both the meridian/radial and transverse directions. The shell/plate is assumed to be supported by a non-uniform Winkler-type elastic foundation in addition to the edge constraints. Therefore, the considered problem contains some complexities that have not been considered together in the available researches. The proposed unified formulation is derived based on the principle of minimum total potential energy and solved using a differential transform analytical method whose center is located at the outer edge of the shell or plate; so that the resulting semi-analytical solution can be employed not only for truncated conical shells and annular plates, but also for complete conical shells and circular plates. Accuracy of results of the proposed unified formulation is verified by comparing the results with those of the three-dimensional theory of elasticity extracted from the ABAQUS finite element analysis code. A variety of the edge condition combinations are considered in the results section. A comprehensive parametric study including assessment of influences of the material properties indices, thickness to radius ratio, stiffness distribution of the elastic foundation, and various boundary conditions, is accomplished. Results reveal that influence of the meridian variations of the material properties on the natural frequencies is more remarkable than that of the transverse gradation.

Keywords: Free vibration; Bidirectional functionally graded; Conical and cylindrical shells; Annular plates; Non-uniform elastic foundation.

1 INTRODUCTION

MANY structural components have been formed in the shape of a shell of revolution. The circular/annular and conical/cylindrical shells are among the common examples of this kind of structures. The main reason for

*Corresponding author.
E-mail address: m.shaban@basu.ac.ir (M. Shaban).

commonly using the motioned structures is the geometrical symmetry; so that more simpler and economic manufacturing processes may be used and less energy dissipation (e.g., heat transfer), coating costs, rotational capability, etc. may be achieved. Using functionally graded material properties enables establishment of a somewhat uniform resulting effective stress to strength ratio in the structure, through accurately tailoring variations of the material properties. Since the stresses of the axisymmetric structures vary in both meridian/radial and thickness directions, a bidirectional functionally graded material should be employed to accomplish the mentioned aim more properly. To this end, proper shell/plate theories may be used to accurately simulate the structure. Various form of the shell theories have been proposed so far. More details may be found in the comprehensive books published by Quta [1], Reddy [2], Shen [3], Carrera et al. [4], and Tornabene and Fantuzzi [5]. The main difference between all of these theories was the form the transverse interpolating function; so that apart from the polynomial, trigonometric, hyperbolic interpolating functions, piecewise defined (layer wise, zigzag, and global-local theories) have been developed. It is evident that last category of theories reduces to the previous category for the single-layer functionally graded shells, unless the thickness is divided to artificial layers. On the other hand, since assumptions of the first-order shear-deformation theories (FSDTs) holds largely in the relatively rigid functionally graded shells, using high-order theories may be neither economic nor more accurate. Results of the FSDT may be especially justified for the global responses. Using higher order approximations (that what really is) may even lead to erroneous results in some situations [2] due to the oscillatory nature of the interpolation functions. Efraim and Eisenberger [6] used exact element method to analyze the vibration of variable thickness annular FGM plates based on FSDT. Hosseini-Hashemi et al. [7] presented an approach for in-plane/out-of-plane free vibration of circular and annular moderately thick FGM plates. Based on 3D elasticity theory, dynamic analysis of multi-directional FGM annular plates was investigated by Nie and Zhong [8] using the state-space-based DQM. Malekzadeh et al. [9] studied free vibration of elastically supported FGM annular plates in thermal environments. Jodaei et al. [10] performed a free vibration analysis for FGM annular plates by the state-space based DQM. Dong [11] presented three- dimensional free vibration analysis of FGM annular plates using Chebyshev–Ritz method. Shariyat and Alipour have presented analytical solutions for free vibration of circular [12-15] and annular [16] transverse/bidirectional elastic/viscoelastic FGM plates with uniform/variable thickness with or without elastic foundations. The fully coupled thermo-mechanical behavior of bi-directional functionally graded material (FGM) beam structures is studied by Lezgy-Nazargah [17]. Free vibration analysis of variable thickness viscoelastic circular plates made of heterogeneous materials was performed by M Shariyat et al. [18]. Free vibration and modal stress analyses of thin circular plates resting on two-parameter elastic foundations were investigated by Alipour et al. [19]. Analysis of functionally graded and layered neutral magneto-electro-elastic plates resting on two-parameter elastic foundations was performed by Lezgy-Nazargah and Cheraghi [20]. Free vibration of FGM plates rested on two-parameter elastic foundations were investigated by Lezgy-Nazargah and Meshkani [21].

In contrast to cylindrical shells [22-31], a few researches may be found in literature on the functionally graded annular plates and conical shells. A finite element formulation based on the FSDT was used by Bhangale et al. [32] to study the thermal buckling and vibration behavior of truncated transversely FGM conical shells in a high-temperature environment, employing a Fourier series expansion for the displacement variable in the circumferential direction. Tornabene [33] and Tornabene et al. [34] presented free vibration analysis for transversely graded conical, cylindrical shell and annular plates, based on the FSDT and the GDQ solution procedure. Qu et al. [35] developed a general formulation for free, steady-state, and transient vibration analyses of transversely graded shells of revolution subjected to arbitrary boundary conditions, using the FSDT. Fourier series and polynomials are applied to expand the displacements and rotations of each shell segment. Free vibration and stability of transversely graded truncated and complete conical shells with free/clamped boundary conditions subjected to external pressures were investigated by Sofiyev [36, 37], using Donnell shell theory, Galerkin method, and the stress function concept. Malekzadeh [38] presented a three-dimensional free vibration analysis for the FGM truncated conical shells subjected to thermal environment, solving the resulting equations by the DQ method. Sofiyev [39] investigated non-linear free vibration of the transversely graded truncated conical shells, using Donnell shell theory and the stress function concept. Najafov and Sofiyev [40] extended this approach by considering a surrounding Pasternak elastic medium. Influences of centrifugal and Coriolis forces and the material parameters on free vibration of rotating transversely graded truncated conical shells subjected to different boundary conditions were investigated by Malekzadeh and Heydarpour [41] based on the FSDT and DQM solution procedure. Sofiyev [42] investigated dynamic buckling truncated conical shells with functionally graded coatings and subjected to axial load in the large deformation. Donnell-Mushtari shell theory, von Karman kinematic non-linearity, and the stress function concepts were used. Sofiyev [43] studied the nonlinear vibration of heterogeneous orthotropic truncated conical shells resting on the Winkler–Pasternak elastic foundations. The formulation was based on the Donnell shell theory and von Karman geometric nonlinearity. The basic equations were reduced to time-dependent geometrical nonlinear differential

equations and solved using homotopic perturbation method. Xie et al. [44] provided a FSDT based solution based on Haar wavelet discretization and Fourier series in the axial and circumferential directions, respectively, for the free vibration analysis of the transversely graded conical shells and annular plates. A unified solution for free vibration analysis of transversely graded cylindrical, conical shells and annular plates with general boundary conditions was presented by Su et al. [45] using the FSDT and Rayleigh–Ritz procedure. Modified Fourier series expressed the displacement and rotation parameters. Su et al. [46] presented a three-dimensional vibration analysis for the mentioned structures, considering arbitrary elastic restraints. Tornabene et al. [47] present a free vibration analysis for free-form doubly curved shell structures using higher-order equivalent single layer theories. The resulting equations are solved by the GDQ method. Based on their previous works, Sofiyev and Kuruoglu [48] studied free vibration of FGM truncated conical shells under mixed boundary conditions.

In the present research, a unified formulation that may be simultaneously used for free vibration analysis of the bidirectional functionally graded conical and cylindrical shells and annular plates on non-uniform Winkler-type elastic foundations is proposed. Gradation of the material properties is assumed to be in both the meridian/radial and transverse directions. The proposed unified formulation is derived based on the principle of minimum total potential energy and solved using a differential transform analytical method whose center is located at the outer edge of the shell/plate. Accuracy of results of the proposed unified formulation is verified by comparing the results with those of the three-dimensional theory of elasticity extracted from the ABAQUS finite element analysis code. A variety of the edge condition combinations are considered and a comprehensive parametric study including assessment of influences of the material properties indices, thickness to radius ratio, stiffness distribution of the elastic foundation, and various boundary conditions, is accomplished.

2 THE UNIFIED FORMULATION

2.1 Description of variations of the material properties and the elastic foundation

Consider a two directional functionally graded conical shell with the length L, constant thickness h, inner and outer radius R_i and R_o, resting on a non-uniform elastic foundation, as shown in Fig. 1. It is assume that the material properties are graded in the meridian and transverse directions.

$$\begin{aligned} E(x,z) &= \left[(E_m - E_c)V_m + E_c\right]\left(\alpha_0 + \alpha_1 x + \alpha_2 x^2\right) \\ \rho(x,z) &= \left[(\rho_m - \rho_c)V_m + \rho_c\right]\left(\beta_0 + \beta_1 x + \beta_2 x^2\right) \end{aligned} \tag{1}$$

where E_c, ρ_c and E_m, ρ_m represent Young's modulus and mass density of the ceramic and metal constituent materials, respectively. V_m is the volume fraction of the ceramic. α_i and β_i (i=1,2,3) are the coefficients of the meridian variations of Young's modulus and mass density, respectively. The ceramic volume fraction is assumed to follow a power–law distribution as:

$$V_m = \left(\frac{1}{2} + \frac{z}{h}\right)^g \tag{2}$$

where g is the positive definite volume fraction index. The elastic foundation is assumed to be a parabolic function; i.e. $k = k_w(\gamma_0 + \gamma_1 x + \gamma_2 x^2)$.

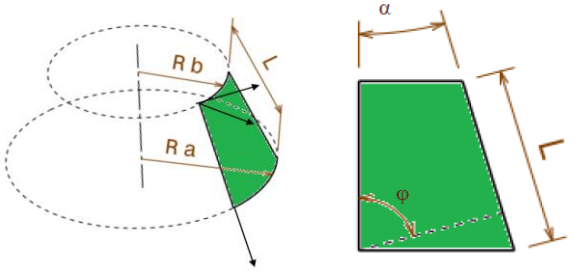

Fig.1
Geometric parameters of the bi-directional FGM conical shell.

2.2 Derivation of the governing equations

Based on the First-order Shear Deformation Theory, the displacement field of axisymmetric shell can be defined as:

$$\begin{aligned} U(x,z,t) &= u_0(x,t) + z\,\psi_x(x,t) \\ W(x,z,t) &= w_0(x,t) \end{aligned} \tag{3}$$

where u_0 and w denote the mid-plane displacements in the x and z directions, respectively. ψ_x is the transverse normal rotation of the normal to the reference surface and t represents the time. For small deflections of conical shells, the strain-displacement relations may be written as:

$$\begin{aligned} &\varepsilon_x = u_{0,x} + z\,\psi_{x,x}, \\ &\varepsilon_\theta = \frac{u_0 Cos(\varphi)}{R_0} + \frac{w Sin(\varphi)}{R_0} + z\,\frac{\psi_x Cos(\varphi)}{R_0}, \\ &\gamma_{xz} = \psi_x + w_{,x} \\ &R_0 = R_b + x Cos(\varphi) \end{aligned} \tag{4}$$

where ε_x and ε_θ are the normal strain components and γ_{xz} indicate the transverse shear strain. R_0 is the radius of the cone in any plane perpendicular to cone axis.

On the other hand, if the transverse normal strain can be neglected, Hooke's generalized stress-strain law may be expressed as:

$$\begin{aligned} \sigma_x &= \frac{E(x,z)}{1-\nu^2}(\varepsilon_x + \nu\,\varepsilon_\theta) = \frac{E(x,z)}{1-\nu^2}\left(u_{0,x} + \nu\,\frac{u_0 Cos(\varphi)}{R_0} + \nu\,\frac{w Sin(\varphi)}{R_0}\right) + \frac{E(x,z)z}{1-\nu^2}\left(\psi_{x,x} + \nu\,\frac{\psi_x}{R_0} Cos(\varphi)\right), \\ \sigma_\theta &= \frac{E(x,z)}{1-\nu^2}(\varepsilon_\theta + \nu\varepsilon_x) = \frac{E(x,z)}{1-\nu^2}\left(\frac{u_0 Cos(\varphi)}{R_0} + \frac{w Sin(\varphi)}{R_0} + \nu u_{0,x}\right) + \frac{E(x,z)z}{1-\nu^2}\left(\frac{\psi_x}{R_0} Cos(\varphi) + \nu\,\psi_{x,x}\right), \\ \tau_{xz} &= \frac{E(x,z)}{2(1+\bar{\nu})}\gamma_{xz} = \frac{E(x,z)}{2(1+\nu)}(\psi_x + w_{,x}) \end{aligned} \tag{5}$$

The governing equations of motion may be derived by using the minimum total potential energy principle.

Employing this principle leads to the following three equations of motion for the plate under consideration in the cylindrical coordinate system (r, θ, z):

$$\delta U = \int_V \left\{ \sigma_x \delta\left(u_{0,x} + z\,\psi_{x,x}\right) + \sigma_\theta \delta\left(\frac{u_0 Cos(\varphi)}{R_0} + \frac{w Sin(\varphi)}{R_0} + z\left(\frac{\psi_x Cos(\varphi)}{R_0}\right)\right) + \tau_{xz}\,\delta\left(\psi_x + w_{,x}\right)\right\} dV \tag{6}$$

$$\delta K = -\int_V \rho\left\{\ddot{U}\,\delta U + \ddot{W}\,\delta W\right\} dV, \tag{7}$$

$$\delta V = \int_V \left[k_w\,(\gamma_0 + \gamma_1 x + \gamma_2 x^2) w\,\delta w \right] dA \tag{8}$$

$$\begin{aligned} &N_{x,x} + \frac{N_x - N_\theta}{R_0} Cos(\varphi) = I_0 \ddot{u}_0 + I_1 \ddot{\psi}_x \\ &M_{x,x} + \frac{M_x - M_\theta}{R_0} Cos(\varphi) - Q_{xz} = I_1 \ddot{u}_0 + I_2 \ddot{\psi}_x \\ &Q_{xz,x} + \frac{Q_{xz}}{R_0} Cos(\varphi) - \frac{N_\theta}{R_0} Sin(\varphi) - k_w\,(\gamma_0 + \gamma_1 x + \gamma_2 x^2) w = I_0 \ddot{w} \end{aligned} \tag{9}$$

Details of derivation of Eq. (9) are not included in the present paper to save space. Based on Eq. (5), The stress resultants M, N, Q are defined as:

$$\begin{aligned}
N_x &= \int_{-h/2}^{h/2} \sigma_x dz = A u_{0,x} + \tilde{A}\frac{Cos(\varphi)}{R_0}u_0 + \tilde{A}\frac{Sin(\varphi)}{R_0}w + B\psi_{x,x} + \tilde{B}\frac{Cos(\varphi)}{R_0}\psi_x \\
N_\theta &= \int_{-h/2}^{h/2} \sigma_\theta dz = A\frac{Cos(\varphi)}{R_0}u_0 + A\frac{Sin(\varphi)}{R_0}w + \tilde{A}u_{0,x} + B\frac{Cos(\varphi)}{R_0}\psi_x + \tilde{B}\psi_{x,x} \\
M_x &= \int_{-h/2}^{h/2} \sigma_x z dz = B u_{0,x} + \tilde{B}\frac{Cos(\varphi)}{R_0}u_0 + \tilde{B}\frac{Sin(\varphi)}{R_0}w + D\psi_{x,x} + \tilde{D}\frac{Cos(\varphi)}{R_0}\psi_x \\
M_\theta &= \int_{-h/2}^{h/2} \sigma_\theta z dz = B\frac{Cos(\varphi)}{R_0}u_0 + B\frac{Sin(\varphi)}{R_0}w + \tilde{B}u_{0,x} + D\frac{Cos(\varphi)}{R_0}\psi_x + \tilde{D}\psi_{x,x}
\end{aligned} \tag{10}$$

$$Q_x = \int_{-h/2}^{h/2} \tau_{xz} dz = \bar{A}\left(\psi_x + w_{,x}\right) \tag{11}$$

where

$$\begin{Bmatrix} A \\ B \\ D \end{Bmatrix} = \int_{-h/2}^{h/2} \frac{E(x,z)}{1-\nu^2}\begin{Bmatrix} 1 \\ z \\ z^2 \end{Bmatrix} dz,\ \begin{Bmatrix} \tilde{A} \\ \tilde{B} \\ \tilde{D} \end{Bmatrix} = \int_{-h/2}^{h/2} \frac{\nu E(x,z)}{1-\nu^2}\begin{Bmatrix} 1 \\ z \\ z^2 \end{Bmatrix} dz,\ \begin{Bmatrix} \bar{A} \\ \bar{B} \\ \bar{D} \end{Bmatrix} = \int_{-h/2}^{h/2} \frac{E(x,z)}{2(1+\nu)}\begin{Bmatrix} 1 \\ z \\ z^2 \end{Bmatrix} dz,$$

$$\begin{Bmatrix} I_0 \\ I_1 \\ I_2 \end{Bmatrix} = \int_{-h/2}^{h/2} \rho(x,z)\begin{Bmatrix} 1 \\ z \\ z^2 \end{Bmatrix} dz$$

$$\begin{cases} A = a_0 + a_1(x-x_0) + a_2(x-x_0)^2 \\ B = b_0 + a_1(x-x_0) + a_2(x-x_0)^2 \\ D = d_0 + d_1(x-x_0) + a_2(x-x_0)^2 \\ \bar{A} = \bar{a}_0 + \bar{a}_1(x-x_0) + \bar{a}_2(x-x_0)^2 \end{cases} \tag{12}$$

$$\begin{cases} I_0 = \bar{I}_0^{(0)} + \bar{I}_0^{(1)}(x-x_0) + \bar{I}_0^{(2)}(x-x_0)^2 \\ I_1 = \bar{I}_1^{(0)} + \bar{I}_1^{(1)}(x-x_0) + \bar{I}_1^{(2)}(x-x_0)^2 \\ I_2 = \bar{I}_2^{(0)} + \bar{I}_2^{(1)}(x-x_0) + \bar{I}_2^{(2)}(x-x_0)^2 \end{cases}$$

The governing Eqs (9) may be simplified and rewritten based on Eqs. (10-12) as:

$$\begin{aligned}
&A u_{0,xx} + A\frac{Cos(\varphi)}{R_0}u_{0,x} - A\frac{Cos^2(\varphi)}{R_0^2}u_0 \\
&+ B\psi_{x,xx} + B\frac{Cos(\varphi)}{R_0}\psi_{x,x} - B\frac{Cos^2(\varphi)}{R_0^2}\psi_x \\
&+ \tilde{A}\frac{Sin(\varphi)}{R_0}w_{,x} - A\frac{Sin(\varphi)Cos(\varphi)}{R_0^2}w \\
&+ A_{,x}u_{0,x} + \tilde{A}_{,x}\frac{Cos(\varphi)}{R_0}u_0 + \tilde{A}_{,x}\frac{Sin(\varphi)}{R_0}w + B_{,x}\psi_{x,x} + \tilde{B}_{,x}\frac{Cos(\varphi)}{R_0}\psi_x = I_0\ddot{u}_0 + I_1\ddot{\psi}_x
\end{aligned} \tag{13a}$$

$$
\begin{aligned}
&Bu_{0,xx}+B\frac{Cos(\varphi)}{R_0}u_{0,x}-B\frac{Cos^2(\varphi)}{R_0^2}u_0\\
&+D\psi_{x,xx}+D\psi_{x,x}\frac{Cos(\varphi)}{R_0}-D\frac{Cos^2(\varphi)}{R_0^2}\psi_x\\
&+\tilde{B}\frac{Sin(\varphi)}{R_0}w_{,x}-B\frac{Sin(\varphi)Cos(\varphi)}{R_0^2}w-\kappa\bar{A}\left(\psi_x+w_{,x}\right)\\
&+B_{,x}u_{0,x}+\tilde{B}_{,x}\frac{Cos(\varphi)}{R_0}u_0+\tilde{B}_{,x}\frac{Sin(\varphi)}{R_0}w+D_{,x}\psi_{x,x}+\tilde{D}_{,x}\frac{Cos(\varphi)}{R_0}\psi_x=I_1\ddot{u}_0+I_2\ddot{\psi}_x
\end{aligned}
\tag{13b}
$$

$$
\begin{aligned}
&-\tilde{A}\frac{Sin(\varphi)}{R_0}u_{0,x}-A\frac{Cos(\varphi)Sin(\varphi)}{R_0^2}u_0\\
&-\frac{Sin(\varphi)}{R_0}\tilde{B}\psi_{x,x}-B\frac{Cos(\varphi)Sin(\varphi)}{R_0^2}\psi_x+\kappa\bar{A}\psi_{x,x}+\bar{A}\frac{Cos(\varphi)}{R_0}\psi_x\\
&+\bar{A}w_{,xx}+\bar{A}\frac{Cos(\varphi)}{R_0}w_{,x}-A\frac{Sin^2(\varphi)}{R_0^2}w\\
&-k_w(\gamma_0+\gamma_1x+\gamma_2x^2)w+\bar{A}_{,x}\left(\psi_x+w_{,x}\right)=I_0\ddot{w}
\end{aligned}
\tag{13c}
$$

2.3 The mathematical forms of the boundary conditions

We consider some most common edge conditions of the solid circular plates to develop the semi-analytical solution:
Roller-supported edge:

$$N_x=0,\ M_x=0,\ w=0, \tag{14a}$$

Free edge:

$$u=0,\ M_r=0,\ w=0, \tag{14b}$$

Clamped edge:

$$u=0,\ \psi_x=0,\ w=0, \tag{14c}$$

3 THE ANALYTICAL DIFFERENTIAL TRANSFORM SOLUTION

By using series solutions for the unknown displacement:

$$
\begin{aligned}
&u_0(x,\theta,t)=\sum_{i=0}^{\infty}U_i(x-x_0)^i\\
&\psi_x(x,\theta,t)=\sum_{i=0}^{\infty}\Psi_i^{(x)}(x-x_0)^i\\
&w(x,\theta,t)=\sum_{i=0}^{\infty}W_i(x-x_0)^i\\
&\frac{Cos(\varphi)}{R_b+x\,Cos(\varphi)}=-\sum_{j=0}^{\infty}\left(-\frac{Cos(\varphi)}{R_b+x_0Cos(\varphi)}\right)^{j+1}(x-x_0)^j\\
&\frac{Cos(\varphi)^2}{\left(R_b+x\,Cos(\varphi)\right)^2}=\sum_{j=0}^{\infty}(j+1)\left(-\frac{Cos(\varphi)}{R_b+x_0Cos(\varphi)}\right)^{j+2}(x-x_0)^j
\end{aligned}
\tag{15}
$$

In practical applications, the functions must be expressed by means of finite series. By substituting Eq. (15) into the governing Eq. (13) and performing some manipulations, the transformed form of Eq. (13) may be obtained as:

$$\begin{aligned}
&\sum_{i=0}^{N}\Bigg\{-\sum_{j=0}^{i+1}(i-j+1)Y^{\,j+1}\left(a_0U_{i-j+1}+b_0\Psi^{(x)}_{i-j+1}+\tan(\varphi)\tilde{a}_0W_{i-j+1}\right)-\sum_{j=0}^{i}(j+1)Y^{\,j+2}\left(a_0U_{i-j}+b_0\Psi^{(x)}_{i-j}+\tan(\varphi)a_0W_{i-j}\right)-\\
&\quad\sum_{j=0}^{i}(i-j)Y^{\,j+1}\left(a_1U_{i-j}+b_1\Psi^{(x)}_{i-j}+\tan(\varphi)\tilde{a}_1W_{i-j}\right)-\sum_{j=0}^{i-1}(j+1)Y^{\,j+2}\left(a_1U_{i-j-1}+b_1\Psi^{(x)}_{i-j-1}+\tan(\varphi)a_1W_{i-j-1}\right)-\\
&\quad\sum_{j=0}^{i-1}(i-j-1)Y^{\,j+1}\left(a_2U_{i-j-1}+b_2\Psi^{(x)}_{i-j-1}+\tan(\varphi)\tilde{a}_2W_{i-j-1}\right)-\sum_{j=0}^{i-2}(j+1)Y^{\,j+2}\left(a_2U_{i-j-2}+b_2\Psi^{(x)}_{i-j-2}+\tan(\varphi)a_2W_{i-j-2}\right)-\\
&\quad\sum_{j=0}^{i}Y^{\,j+1}\left(\tilde{a}_1U_{i-j}+\tilde{b}_1\Psi^{(x)}_{i-j}+\tan(\varphi)\tilde{a}_1W_{i-j}\right)-\sum_{j=0}^{i-1}Y^{\,j+1}\left(\tilde{a}_2U_{i-j-1}+\tilde{b}_2\Psi^{(x)}_{i-j-1}+\tan(\varphi)\tilde{a}_2W_{i-j-1}\right)+\\
&\quad(i+2)(i+1)\left(a_0U_{i+2}+b_0\Psi^{(x)}_{i+2}\right)+(i+1)^2\left(a_1U_{i+1}+b_1\Psi^{(x)}_{i+1}\right)+i(i+1)\left(a_2U_i+b_2\Psi^{(x)}_i\right)+\\
&\quad\omega^2\left(\bar{I}^{(0)}_0U_i+\bar{I}^{(1)}_0U_{i-1}+\bar{I}^{(2)}_0U_{i-2}\right)+\omega^2\left(\bar{I}^{(0)}_1\Psi^{(x)}_i+\bar{I}^{(1)}_1\Psi^{(x)}_{i-1}+\bar{I}^{(2)}_1\Psi^{(x)}_{i-2}\right)\Bigg]\Bigg\}(x-x_0)^i=0
\end{aligned}\tag{16a}$$

$$\begin{aligned}
&\sum_{i=0}^{N}\Bigg\{-\sum_{j=0}^{i+1}Y^{\,j+1}(i-j+1)\left(b_0U_{i-j+1}+d_0\Psi^{(x)}_{i-j+1}+\tan(\varphi)\tilde{b}_0W_{i-j+1}\right)-\sum_{j=0}^{i}(j+1)Y^{\,j+2}\left(b_0U_{i-j}+d_0\Psi^{(x)}_{i-j}+b_0\tan(\varphi)W_{i-j}\right)-\\
&\quad\sum_{j=0}^{i}Y^{\,j+1}(i-j)\left(b_1U_{i-j}+d_1\Psi^{(x)}_{i-j}+\tan(\varphi)\tilde{b}_1W_{i-j}\right)-\sum_{j=0}^{i-1}(j+1)Y^{\,j+2}\left(b_1U_{i-j-1}+d_1\Psi^{(x)}_{i-j-1}+b_1\tan(\varphi)W_{i-j-1}\right)-\\
&\quad\sum_{j=0}^{i-1}Y^{\,j+1}(i-j-1)\left(b_2U_{i-j-1}+d_2\Psi^{(x)}_{i-j-1}+\tan(\varphi)\tilde{b}_2W_{i-j-1}\right)-\sum_{j=0}^{i-2}(j+1)Y^{\,j+2}\left(b_2U_{i-j-2}+d_2\Psi^{(x)}_{i-j-2}+b_2\tan(\varphi)W_{i-j-2}\right)-\\
&\quad\sum_{j=0}^{i}Y^{\,j+1}\left(\tilde{b}_1U_{i-j}+\tilde{d}_1\Psi^{(x)}_{i-j}+\tan(\varphi)\tilde{b}_1W_{i-j}\right)-2\sum_{j=0}^{i-1}Y^{\,j+1}\left(\tilde{b}_2U_{i-j-1}+\tilde{d}_2\Psi^{(x)}_{i-j-1}+\tan(\varphi)\tilde{b}_2W_{i-j-1}\right)+\\
&\quad(i+2)(i+1)\left(a_0U_{i+2}+b_0\Psi^{(x)}_{i+2}\right)+(i+1)^2\left(b_1U_{i+1}+d_1F_{i+1}\right)+i(i+1)\left(b_2U_i+d_2\Psi^{(x)}_i\right)-\\
&\quad\bar{a}_0\left(\Psi^{(x)}_i+(i+1)W_{i+1}\right)-\bar{a}_1\left(\Psi^{(x)}_{i-1}+(i-1)W_{i-1}\right)-\bar{a}_2\left(\Psi^{(x)}_{i-2}+(i-2)W_{i-2}\right)+\\
&\quad\omega^2\left(\bar{I}^{(0)}_1U_i+\bar{I}^{(1)}_1U_{i-1}+\bar{I}^{(2)}_1U_{i-2}\right)+\omega^2\left(\bar{I}^{(0)}_2\Psi^{(x)}_i+\bar{I}^{(1)}_2\Psi^{(x)}_{i-1}+\bar{I}^{(2)}_2\Psi^{(x)}_{i-2}\right)\Bigg\}(x-x_0)^i=0
\end{aligned}\tag{16b}$$

$$\begin{aligned}
&\sum_{i=0}^{N}\Bigg\{\tan(\varphi)\sum_{j=0}^{i+1}Y^{\,j+1}(i-j+1)\left(\tilde{a}_0U_{i-j+1}+\tilde{b}_0\Psi^{(x)}_{i-j+1}\right)+\tan(\varphi)\sum_{j=0}^{i}Y^{\,j+1}(i-j)\left(\tilde{a}_1U_{i-j}+\tilde{b}_1\Psi^{(x)}_{i-j}\right)+\\
&\quad\tan(\varphi)\sum_{j=0}^{i-1}Y^{\,j+1}(i-j-1)\left(\tilde{a}_2U_{i-j-1}+\tilde{b}_2\Psi^{(x)}_{i-j-1}\right)-\tan(\varphi)\sum_{j=0}^{i}(j+1)Y^{\,j+2}\left(a_0U_{i-j}+b_0\Psi^{(x)}_{i-j}\right)-\\
&\quad\tan(\varphi)\sum_{j=0}^{i-1}jY^{\,j+2}\left(a_1U_{i-j-1}+b_1\Psi^{(x)}_{i-j-1}\right)-\tan(\varphi)\sum_{j=0}^{i-2}(j+1)Y^{\,j+2}\left(a_2U_{i-j-2}+b_2\Psi^{(x)}_{i-j-2}\right)-\\
&\quad\bar{a}_0\sum_{j=0}^{i+1}Y^{\,j+1}(i-j+1)W_{i-j+1}-\bar{a}_1\sum_{j=0}^{i}Y^{\,j+1}(i-j)W_{i-j}-\bar{a}_2\sum_{j=0}^{i-1}Y^{\,j+1}(i-j-1)W_{i-j-1}-\bar{a}_0\sum_{j=0}^{i}Y^{\,j+1}\Psi^{(x)}_{i-j}-\\
&\quad\bar{a}_1\sum_{j=0}^{i_1-1}Y^{\,j+1}\Psi^{(x)}_{i-j-1}-\bar{a}_2\sum_{j=0}^{i-2}Y^{\,j+1}\Psi^{(x)}_{i-j-2}+\bar{a}_0(i+1)\Psi^{(x)}_{i+1}+\bar{a}_1i\Psi^{(x)}_i+\bar{a}_2(i-1)\Psi^{(x)}_{i-1}+\bar{a}_0(i+1)(i+2)W_{i+2}+\\
&\quad\bar{a}_1i(i+1)W_{i+1}+\bar{a}_2(i-1)iW_i-_0\tan^2(\varphi)\sum_{j=0}^{i}(j+1)Y^{\,j+2}W_{i-j}-aa_1\tan^2(\varphi)\sum_{j=0}^{i-1_1}(j+1)Y^{\,j+2}W_{i-j-1}-\\
&\quad a_2\tan^2(\varphi)\sum_{j=0}^{i-2}(j+1)Y^{\,j+2}W_{i-j-2}+\bar{a}_1\left(\Psi^{(x)}_i+(i+1)W_{i+1}\right)+2\bar{a}_2\left(\Psi^{(x)}_{i-1}+iW_i\right)-\\
&\quad k_w\left[\left(\gamma_0+\gamma_1b+\gamma_2b^2\right)W_i+\left(\gamma_1+2\gamma_2b\right)W_{i-1}+\gamma_2W_{i-2}\right]+\omega^2\left(\bar{I}^{(0)}_0W_i+\bar{I}^{(1)}_0W_{i-1}+\bar{I}^{(2)}_0W_{i-2}\right)\Bigg\}(x-x_0)^i=0
\end{aligned}\tag{16c}$$

By substituting Eq. (15) into the boundary condition Eq. (14), the transformed form of Eq. (14) may be written as:

$$
\begin{aligned}
N_x &= \sum_{i=0}^{N}\Bigg[a_0(i+1)U_{i+1}+a_1 iU_i+a_2(i-1)U_{i-1}+\frac{Cos(\varphi)}{R_0}\left(\tilde{a}_0U_i+\tilde{a}_1U_{i-1}+\tilde{a}_2U_{i-2}\right)+\\
&\quad \frac{Sin(\varphi)}{R_0}\left(\tilde{a}_0W_i+\tilde{a}_1W_{i-1}+\tilde{a}_2W_{i-2}\right)+b_0(i+1)\Psi_{i+1}^{(x)}+b_1 i\,\Psi_i^{(x)}+b_2(i-1)\Psi_{i-1}^{(x)}+\\
&\quad +\frac{Cos(\varphi)}{R_0}\left(\tilde{b}_0\Psi_i^{(x)}+\tilde{b}_1\Psi_{i-1}^{(x)}+\tilde{b}_2\Psi_{i-2}^{(x)}\right)\Bigg](x-x_0)^i=0\\
M_x &= \sum_{i=0}^{N}\Big[b_0(i+1)U_{i+1}+b_1 iU_i+b_2(i-1)U_{i-1}+\frac{Cos(\varphi)}{R_0}\left(\tilde{b}_0U_i+\tilde{b}_1U_{i-1}+\tilde{b}_2U_{i-2}\right)+\\
&\quad \frac{Sin(\varphi)}{R_0}\left(\tilde{b}_0W_i+\tilde{b}_1W_{i-1}+\tilde{b}_2W_{i-2}\right)+d_0(i+1)\Psi_{i+1}^{(x)}+d_1 i\,\Psi_i^{(x)}+d_2(i-1)\Psi_{i-1}^{(x)}+\\
&\quad \frac{Cos(\varphi)}{R_0}\left(\tilde{d}_0\Psi_i^{(x)}+\tilde{d}_1\Psi_{i-1}^{(x)}+\tilde{d}_2\Psi_{i-2}^{(x)}\right)\Big](x-x_0)^i=0\\
Q_x &= \sum_{i=0}^{N}\left\{\kappa\bar{a}_0\left[\Psi_i^{(x)}+(i+1)W_{i+1}\right]+\kappa\bar{a}_1\left(\Psi_{i-1}^{(x)}+iW_i\right)+\kappa\bar{a}_2\left[\Psi_{i-2}^{(x)}+(i-1)W_{i-1}\right]\right\}(x-x_0)^i=0
\end{aligned}
\tag{17}
$$

Obtaining Taylor's series expansion of the dimensionless displacements based on Eq. (16) and substituting the resulted expression into the boundary conditions (17), the resulted equations can be expressed in the following matrix form:

$$
\begin{bmatrix}
\chi_{11}^{(N)} & \chi_{12}^{(N)} & \chi_{13}^{(N)} & \chi_{14}^{(N)} & \chi_{15}^{(N)} & \chi_{16}^{(N)}\\
\chi_{21}^{(N)} & \chi_{22}^{(N)} & \chi_{23}^{(N)} & \chi_{24}^{(N)} & \chi_{25}^{(N)} & \chi_{26}^{(N)}\\
\chi_{31}^{(N)} & \chi_{32}^{(N)} & \chi_{33}^{(N)} & \chi_{34}^{(N)} & \chi_{35}^{(N)} & \chi_{36}^{(N)}\\
\chi_{41}^{(N)} & \chi_{42}^{(N)} & \chi_{43}^{(N)} & \chi_{44}^{(N)} & \chi_{45}^{(N)} & \chi_{46}^{(N)}\\
\chi_{51}^{(N)} & \chi_{52}^{(N)} & \chi_{53}^{(N)} & \chi_{54}^{(N)} & \chi_{55}^{(N)} & \chi_{56}^{(N)}\\
\chi_{61}^{(N)} & \chi_{62}^{(N)} & \chi_{63}^{(N)} & \chi_{64}^{(N)} & \chi_{65}^{(N)} & \chi_{66}^{(N)}
\end{bmatrix}
\begin{Bmatrix} U_0\\ U_1\\ \Psi_0\\ \Psi_1\\ W_0\\ W_1 \end{Bmatrix}
=\begin{Bmatrix} 0\\0\\0\\0\\0\\0 \end{Bmatrix}
\tag{18}
$$

where χ_{ij} are polynomials in terms of Ωcorresponding to nth term.

Existence condition of the non-trivial solutions yields the following characteristic determinant:

$$
\begin{vmatrix}
\chi_{11}^{(N)} & \chi_{12}^{(N)} & \chi_{13}^{(N)} & \chi_{14}^{(N)} & \chi_{15}^{(N)} & \chi_{16}^{(N)}\\
\chi_{21}^{(N)} & \chi_{22}^{(N)} & \chi_{23}^{(N)} & \chi_{24}^{(N)} & \chi_{25}^{(N)} & \chi_{26}^{(N)}\\
\chi_{31}^{(N)} & \chi_{32}^{(N)} & \chi_{33}^{(N)} & \chi_{34}^{(N)} & \chi_{35}^{(N)} & \chi_{36}^{(N)}\\
\chi_{41}^{(N)} & \chi_{42}^{(N)} & \chi_{43}^{(N)} & \chi_{44}^{(N)} & \chi_{45}^{(N)} & \chi_{46}^{(N)}\\
\chi_{51}^{(N)} & \chi_{52}^{(N)} & \chi_{53}^{(N)} & \chi_{54}^{(N)} & \chi_{55}^{(N)} & \chi_{56}^{(N)}\\
\chi_{61}^{(N)} & \chi_{62}^{(N)} & \chi_{63}^{(N)} & \chi_{64}^{(N)} & \chi_{65}^{(N)} & \chi_{66}^{(N)}
\end{vmatrix}=0
\tag{19}
$$

4 RESULTS AND DISCUSSIONS

The numerical results are tabulated in Tables 1–9 and illustrated in Figs. 2-3 for bidirectional functionally graded conical/cylindrical shells and annular plates resting on elastic foundation under different boundary conditions. In order to validate the present analysis, finite element (FE) simulations via commercially available FE code ABAQUS are undertaken in all tables for annular, cylindrical and conical shells and compared with obtained results. A 20-node brick element with parabolic basis function C3D20R, which yields more accurate stresses than shell elements in the

thickness direction, is used. Comparison shows excellent agreement between the results from these tables and maximum error is less than 3%. The dependence of natural frequencies on the geometrical parameters, e.g. R_i/R_o and h for annular plates, R and h for cylindrical shells, R, h and φ for conical shells is presented in Tables 1-3. The Young's modulus varies linearly with thickness coordinate. From Table 1, it is observed that the increase of the R_i/R_o ratio yields an increase in the ω_i (i=1, 2, 3) but the fundamental frequency, ω_1 affected more significantly. Similar results also can be concluded for cylindrical and conical shells in Table 2 and 3 by increasing radius or φ. In addition, the effect of thickness is more notable compared to radius. Similar results can be observed for conical/cylindrical shells and annular plates with linear variation of density and Young's modulus in x-direction in Tables 4-6. It is obvious from these tables that when the thickness increases, ω_i increases. Moreover, the restriction of edge increased due to change of boundary conditions from free-end to simply-supported or from simply-supported to clamped edge; hence it leads to highest natural frequencies.

Table 1
First three natural frequencies of foundationless bidirectional annular FGM plates with different boundary conditions and inner to outer radius ratios ($g = 1$, $\gamma_i = 0$, $\alpha_0 = \beta_0 = 1$, $\alpha_{1,2} = \beta_{1,2} = 0$).

Boundary Condition	Frequency (Hz)	h=0.1 R_i/R_o=0.1			h=0.2 R_i/R_o =0.1			h=0.2 R_i/R_o =0.2		
		Present	3D (ABAQUS)	Difference (%)	Present	3D (ABAQUS)	Difference (%)	Present	3D (ABAQUS)	Difference (%)
Annular										
C-C	ω_1	922.47	925.62	0.34	1518.9	1540.2	1.39	1868.2	1898	1.55
	ω_2	2346.5	2363.5	0.72	3467.1	3541.4	2.1	4146.8	4248	2.37
	ω_3	4223.8	4272.2	1.13	5461.8	5436.5	0.47	5868	5850	0.32
C-S	ω_1	618.92	618.13	0.13	1068.7	1076.5	0.73	1345.2	1357	0.86
	ω_2	1954.9	1961.5	0.34	2918	2873.6	1.55	3079.6	3038	1.38
	ω_3	2921.9	2877.2	1.55	3065.4	3113.3	1.54	3730.8	3799	1.79
S-C	ω_1	786.04	790.72	0.59	1401.4	1382	1.4	1601.8	1619	1.08
	ω_2	2128.7	2144	0.71	3356.4	3383.6	0.8	3930.8	4007	1.89
	ω_3	3976.2	4017	1.02	5759.6	5840	1.38	4568.9	4585	0.34
C-F	ω_1	154.23	153.26	0.63	293.34	292.55	0.27	359.69	359	0.2
	ω_2	863.94	862.71	0.14	1443.6	1453.7	0.7	1799.5	1815	0.84
	ω_3	2353.6	2361.6	0.34	2924.6	2878.2	1.61	3091.8	3047	1.48
F-C	ω_1	364.82	366.2	0.38	686.23	691.49	0.76	704.97	709.9	0.7
	ω_2	1347.1	1355.5	0.62	2279.7	2310.6	1.34	2429.2	2460	1.25
	ω_3	2871.9	2897.3	0.88	4405.6	4491.3	1.91	4568.6	4574	0.11

Table 2
First three natural frequencies of foundationless bidirectional cylindrical FGM plates with different boundary conditions and inner to outer radius ratios ($h=0.1$, $g = 1$, $\gamma_i = 0$, $\alpha_0 = \beta_0 = 1$, $\alpha_{1,2} = \beta_{1,2} = 0$).

Boundary Condition	Frequency (Hz)	R=L=1			R=1,L=2			R=L=2		
		Present	3D (ABAQUS)	Difference (%)	Present	3D (ABAQUS)	Difference (%)	Present	3D (ABAQUS)	Difference (%)
Cylindrical										
C-C	ω_1	1571.4	1584.4	0.82	1378.5	1392.5	1.01	712.97	716.21	0.45
	ω_2	2392.8	2408.5	0.65	1415	1424	0.63	860.6	863.29	0.31
	ω_3	3858.4	3893.6	0.9	1694.3	1705	0.62	1243.7	1248.4	0.38
C-S	ω_1	1414.9	1424	0.64	1013	1010.5	0.24	668.56	671.1	0.38
	ω_2	2091.1	2095.7	0.22	1368	1378.8	0.78	799.03	801.03	0.25
	ω_3	2250.8	2254.9	0.18	1443.7	1455.7	0.82	1090.2	1090.5	0.03
S-S	ω_1	1370.2	1380.4	0.74	1298	1309.9	0.91	663.37	670	0.99
	ω_2	1909.1	1915	0.31	1377.1	1380.4	0.24	753.22	757.75	0.6
	ω_3	3187.1	3201	0.44	1525.7	1551.6	1.67	1029.6	1037.2	0.73
C-F	ω_1	1317.2	1329.5	0.93	1012.6	1010.2	0.24	657.35	660.47	0.47
	ω_2	1514.6	1524.3	0.63	1322.7	1336.1	1	686.26	688.95	0.39
	ω_3	2171.8	2170.8	0.05	1384.8	1396.6	0.84	857.11	859.31	0.26

Table 3
First three natural frequencies of foundationless bidirectional conical FGM plates with different boundary conditions and inner to outer radius ratios ($h=0.1$, $g = 1$, $\gamma_i = 0$, $\alpha_0 = \beta_0 = 1$, $\alpha_{1,2} = \beta_{1,2} = 0$).

Boundary Condition		Frequency (*Hz*)	*R*=*L*=1			*R*=1,*L*=2			*R*=*L*=2		
			Present	3D (ABAQUS)	Difference (%)	Present	3D (ABAQUS)	Difference (%)	Present	3D (ABAQUS)	Difference (%)
Conical											
C-C	$\varphi=\pi/6$	ω_1	909.009	913.73	0.52	412.11	413.19	0.26	312.51	313.17	0.21
		ω_2	2047.621	2063.3	0.76	662.97	665.01	0.31	597.03	598.97	0.32
		ω_3	3643.951	3681.6	1.02	1115.2	1119.8	0.41	1073.3	1078	0.43
	$\varphi=\pi/4$	ω_1	1052.829	1058.3	0.52	585.02	587.16	0.36	409.16	410.15	0.24
		ω_2	2114.614	2129.9	0.72	792.61	795.17	0.32	652.44	654.36	0.29
		ω_3	3684.975	3722	0.99	1202.3	1206.9	0.38	1106.7	1111.2	0.4
	$\varphi=\pi/3$	ω_1	1222.592	1222.1	0.27	788.29	792.25	0.5	513.06	514.62	0.3
		ω_2	2199.743	2210.7	0.28	958.98	962.78	0.39	719.48	721.53	0.28
		ω_3	3737.157	3771	0.54	1322.4	1327.4	0.38	1148.8	1153.2	0.38
F-C	$\varphi=\pi/6$	ω_1	579.6134	581.19	0.04	398.95	399.97	0.25	275.51	276	0.18
		ω_2	961.9995	964.67	0.5	512.29	513.33	0.2	337.75	338.19	0.13
		ω_3	2126.474	2138	0.9	719.73	720.99	0.17	614.84	616.14	0.21
	$\varphi=\pi/4$	ω_1	827.609	825.04	0.31	580.96	583.01	0.35	392.13	393.1	0.25
		ω_2	1103.661	1102.2	0.13	703.72	705.91	0.31	445.84	446.78	0.21
		ω_3	2181.32	2189.8	0.39	879.65	881.91	0.26	670.7	672.03	0.2
	$\varphi=\pi/3$	ω_1	1052.594	1048.3	0.41	786.8	790.75	0.5	501.18	502.72	0.31
		ω_2	1257.304	1253.4	0.31	889.57	892.8	0.36	548.82	550.56	0.32
		ω_3	2230.887	2234.5	0.16	1055.01	1059	0.38	735.05	736.61	0.21

Table 4
First three frequencies of annular plate for difference thickness values ($g = 0$, $\gamma_i = 0$, $E = E_m + (E_c - E_m)\frac{x}{L}$, $\rho = \rho_m + (\rho_c - \rho_m)\frac{x}{L}$).

Boundary Condition		Frequency (*Hz*)	R_i/R_o=0.1			*Ri/Ro*=0.2			R_i/R_o=0.5		
			Present	3D (ABAQUS)	Difference (%)	Present	3D (ABAQUS)	Difference (%)	Present	3D (ABAQUS)	Difference (%)
Annular											
C-C	*h*=0.1	ω_1	931.95	939.65	0.82	1165.6	1176.9	0.96	2626.5	2667	1.52
		ω_2	2350.2	2374.5	1.02	2887.7	2922.3	1.18	5978.1	6092	1.87
		ω_3	4199.8	4253.2	1.26	5078	5151.7	1.43	8395.2	8480.3	1
	h=0.2	ω_1	1486.2	1508.3	1.46	1823.6	1853.3	1.6	3596.7	3681.5	2.3
		ω_2	3406.8	3471.6	1.87	4047	4132	2.06	7335.4	7558.3	2.95
		ω_3	5355.7	5385.6	0.56	5673.4	5722.7	0.86	8395.2	8502	1.26
S-C	*h*=0.1	ω_1	821.79	822.42	0.08	989.47	990.1	0.06	2224.8	2235.9	0.49
		ω_2	2195.5	2204.2	0.39	2664.3	2678.9	0.54	5502.7	5490.6	0.22
		ω_3	4050.3	4080.8	0.75	4485	4483.1	0.04	5667	5736.4	1.21
	h=0.2	ω_1	1394.7	1402.9	0.59	1670.7	1681.7	0.65	3352.2	3399.4	1.39
		ω_2	3353.2	3397.7	1.31	3971.4	4032	1.5	5502.7	5493.9	0.16
		ω_3	4841.2	4866	0.51	4485	4482	0.07	7324.2	7496.5	2.3
F-C	*h*=0.1	ω_1	428.28	429.15	0.2	446.88	446.72	0.04	810.21	808.73	0.18
		ω_2	1437.9	1442.3	0.3	1586.7	1588.3	0.1	3240.2	3257.3	0.52
		ω_3	2979.1	2995.9	0.56	3427.3	3445.2	0.52	5502.7	5489.4	0.24
	h=0.2	ω_1	800.89	805.02	0.51	834.86	837.09	0.27	1449	1452	0.2
		ω_2	2405.3	2428.3	0.95	2613.8	2634.5	0.78	4697.7	4766.7	1.45
		ω_3	4500	4563.7	1.4	4485	4478.4	0.15	5502.7	5492.2	0.19

Table 5

First three frequencies of Cylindrical shell for difference thickness and radius values ($L=1$, $g = 0$, $\gamma_i = 0$, $E = E_m + (E_c - E_m)\frac{x}{L}$, $\rho = \rho_m + (\rho_c - \rho_m)\frac{x}{L}$).

Boundary Condition	Frequency (*Hz*)	h=0.1 R=1			h=0.2 R=1			h=0.2 R=2		
		Present	3D (ABAQUS)	Difference (%)	Present	3D (ABAQUS)	Difference (%)	Present	3D (ABAQUS)	Difference (%)
Cylindrical										
C-C	ω_1	1525.8	1528.1	0.15	1849.2	1858.2	0.48	1465.8	1479.8	0.95
	ω_2	2350.8	2359.9	0.38	3206.3	3241.4	1.08	3042.2	3089.2	1.52
	ω_3	3794.2	3825.6	0.82	4102.5	4137.2	0.84	4079.3	4113.8	0.84
C-S	ω_1	1354.1	1351.6	0.18	1612.6	1608.2	0.28	1238.8	1239.9	0.09
	ω_2	2127.1	2128.1	0.05	2499.3	2495	0.17	2481.6	2475.1	0.26
	ω_3	2533	2519.4	0.54	3081.6	3091	0.31	2875.5	2901.5	0.89
S-S	ω_1	1323.7	1322.1	0.12	1452.4	1445.1	0.5	952.75	949.19	0.38
	ω_2	1902	1895.3	0.35	2701.4	2695	0.24	2482	2491.2	0.37
	ω_3	3196.8	3196.3	0.01	4250.7	4236.7	0.33	4234.9	4219.3	0.37
C-F	ω_1	1017	1021.4	0.43	1076.3	1085	0.81	619.88	621.23	0.22
	ω_2	1493	1490.7	0.15	1913.3	1912.1	0.06	1641.1	1645.6	0.27
	ω_3	2414.8	2418	0.13	2524.6	2515.7	0.35	2487.7	2479.6	0.33

Table 6

First three frequencies of Conical shell for difference thickness and radius values ($L=1$, $g = 0$, $\gamma_i = 0$, $E = E_m + (E_c - E_m)\frac{x}{L}$, $\rho = \rho_m + (\rho_c - \rho_m)\frac{x}{L}$).

Boundary Condition		Frequency (*Hz*)	h=0.1 R=1			h=0.2 R=1			h=0.2 R=2		
			Present	3D (ABAQUS)	Difference (%)	Present	3D (ABAQUS)	Difference (%)	Present	3D (ABAQUS)	Difference (%)
Conical											
C-C	$\varphi = \pi/6$	ω_1	912.75	916.72	0.43	1394.6	1409.4	1.05	1342.6	1359.5	1.24
		ω_2	2043.7	2061.9	0.88	3019.6	3068.5	1.59	2998.8	3049.7	1.67
		ω_3	3615.2	3656.7	1.14	4181.7	4221.8	0.95	4119.6	4157.7	0.92
	$\varphi = \pi/4$	ω_1	1051.2	1053.5	0.21	1488.3	1499.9	0.77	1373.4	1389.3	1.14
		ω_2	2101.6	2117.9	0.77	3055.9	3101.1	1.46	3009.8	3059.8	1.63
		ω_3	3647.9	3687.4	1.07	4162.7	4202.2	0.94	4110.5	4148.2	0.91
	$\varphi = \pi/3$	ω_1	1213.2	1214.2	0.08	1605.4	1614.4	0.56	1409	1423.8	1.04
		ω_2	2176.6	2190.6	0.64	3102.8	3144.5	1.33	3022.6	3071.1	1.58
		ω_3	3691.1	3728.1	0.99	4138.8	4177.7	0.93	4099.5	4136.4	0.89
F-C	$\varphi = \pi/6$	ω_1	495.23	494.72	0.1	598.47	595.67	0.47	440.11	438.75	0.31
		ω_2	1022.8	1021.4	0.14	1667.3	1672.1	0.28	1593.9	1600.9	0.44
		ω_3	2245	2251.6	0.29	2710.9	2703.9	0.26	2582.9	2575.7	0.28
	$\varphi = \pi/4$	ω_1	684.46	684.55	0.01	758.16	755.41	0.36	502.12	500.92	0.24
		ω_2	1128.1	1125.6	0.22	1722.1	1724.1	0.12	1608.7	1614.8	0.38
		ω_3	2288.1	2293.4	0.23	2663.4	2656.4	0.27	2561.9	2554.7	0.28
	$\varphi = \pi/3$	ω_1	848.59	849.78	0.14	907.91	907.12	0.09	560.45	559.77	0.12
		ω_2	1254.5	1251.1	0.27	1790.6	1790.1	0.03	1624.6	1629.8	0.32
		ω_3	2342.1	2346.6	0.19	2605.2	2598.1	0.27	2536.5	2529	0.3

The effect of non-homogeneity material and density parameters in the x-direction are tabulated in Table 7 for different values of α_i and β_i. The nonlinearity of elastic modulus and density increased by considering more coefficients. It is evident from this table that natural frequencies take larger values, provided that either Young's modulus coefficients, α_i or density coefficients, β_i, increase.

Table 7
Effect of non-homogeneity of material in the *x*-direction on the natural frequencies ($R = L = 1$, $g = 0$ *(Al)*, $\gamma_i = 0$, $h = 0.1$).

Freq.			$\alpha_0=\alpha_1=1,\ \alpha_2=0$ $\beta_0=\beta_1=1,\ \beta_2=0$			$\alpha_0=\alpha_1=\alpha_2=1$ $\beta_0=\beta_1=1,\ \beta_2=0$			$\alpha_0=\alpha_1=1,\ \alpha_2=5$ $\beta_0=\beta_1=\beta_2=1$		
			C-C	S-C	F-C	C-C	S-C	F-C	C-C	S-C	F-C
Annular Plate	ω_1	Present	510.79	393.36	128.98	560.39	434.87	148.27	650.73	520.02	199.75
		3D (ABAQUS)	517.46	395.89	129.51	567.54	437.43	148.78	658.82	522.74	200.28
		Difference (%)	1.2896	0.6394	0.4059	1.2602	0.5862	0.3442	1.2275	0.5202	0.2623
	ω_2	Present	1304.6	1135.7	582.59	1424.7	1244.3	644.59	1633.8	1442	775.64
		3D (ABAQUS)	1325	1146.1	586.24	1446.6	1255	648.23	1658.5	1453.6	779.38
		Difference (%)	1.5386	0.9095	0.6229	1.5162	0.8522	0.5618	1.492	0.7954	0.4792
	ω_3	Present	2347.2	1728	1409.4	2558	1933.7	1544.1	2915.9	2425.1	1792.6
		3D (ABAQUS)	2389.9	1732.7	1421.9	2604	1937.9	1556.9	2967.7	2428.1	1806.2
		Difference (%)	1.7851	0.2737	0.8821	1.7651	0.2168	0.8221	1.7449	0.1256	0.7515
Conical Shell $\pi/4$	ω_1	Present	674.73	596.2	518.16	736.8	647.5	539.74	851.84	750.63	584.99
		3D (ABAQUS)	678.75	596.83	517.95	741.06	647.92	539.4	856.63	750.76	584.63
		Difference (%)	0.5922	0.1048	0.0404	0.5748	0.0655	0.0639	0.5595	0.0171	0.0623
	ω_2	Present	1371.3	1207.6	732.32	1495.9	1321.2	796.39	1714	1528.8	932.93
		3D (ABAQUS)	1388.8	1215.1	733.31	1514.7	1328.9	797.29	1735.2	1536.8	933.79
		Difference (%)	1.2583	0.6211	0.135	1.2385	0.5764	0.1131	1.2197	0.5226	0.0924
	ω_3	Present	2386.3	1667	1465.6	2599.7	1871.2	1602.9	2962	2361.3	1856.6
		3D (ABAQUS)	2426.1	1671.6	1475.4	2642.5	1875.2	1612.7	3010.4	2364.2	1866.8
		Difference (%)	1.6406	0.2758	0.662	1.6205	0.2115	0.6102	1.6075	0.1215	0.5484
Cylindrical Shell	ω_1	Present	983.011	878.68	810.19	1064.2	943.76	830.37	1214.8	1075.8	874.19
		3D (ABAQUS)	984.39	877.41	811.35	1065.9	942.22	831.99	1217.5	1074.3	876.67
		Difference (%)	0.1401	0.1444	0.1431	0.161	0.1633	0.1947	0.2187	0.1439	0.2829
	ω_2	Present	1524	1362.9	960.44	1660.1	1488.1	1038.7	1900.2	1721.5	1203.9
		3D (ABAQUS)	1535.5	1364.8	959.99	1672.6	1489.9	1037.7	1914.5	1723.3	1202.4
		Difference (%)	0.7481	0.1416	0.0466	0.745	0.1181	0.0952	0.7477	0.1018	0.1252
	ω_3	Present	2479.6	1576.8	1526.6	2699.8	1779	1692.6	3073.5	2259.4	1991.4
		3D (ABAQUS)	2513	1581.3	1530.8	2735.7	1783	1696.4	3114.2	2262.5	1995.3
		Difference (%)	1.3287	0.2847	0.2762	1.3126	0.2245	0.2251	1.3058	0.1362	0.1941

In Table 8, the variation of E and ρ in thickness direction is studied, by considering different values of g. it is seen that the natural frequencies increases with the increase of power variation, g. It can be also inferred that the effect of parameter g is less pronounced compared to parameters α_i and β_i. As it is expected, the natural frequencies increases as higher degrees of restraints are applied to the plate edges (from simply- supported to clamped edge).

The effect of the foundation stiffness, k_w on the first two natural frequencies are plotted in Figs. 2 and 3 for clamped-clamped and clamped-free boundary conditions, respectively. The results obtained for annular, conical and cylindrical shells. Generally, the annular plate has the smallest ω_i and cylindrical shell has the greater one and natural frequencies of conical shells lays between them. From these figures, one can see that increase in the stiffness of foundation lead to less changes in the vibration behavior than the smooth ones, and the frequency parameters ω_i increase. For conical shell, one can obtain that by increasing the angle φ, the ω_i will be increase. In fact, the lower and upper limit of φ is *0* and $\pi/2$ which coincide with annular and cylindrical shell. As expected, the frequencies for clamped-clamped boundary condition are larger than those for clamped-free boundary condition.

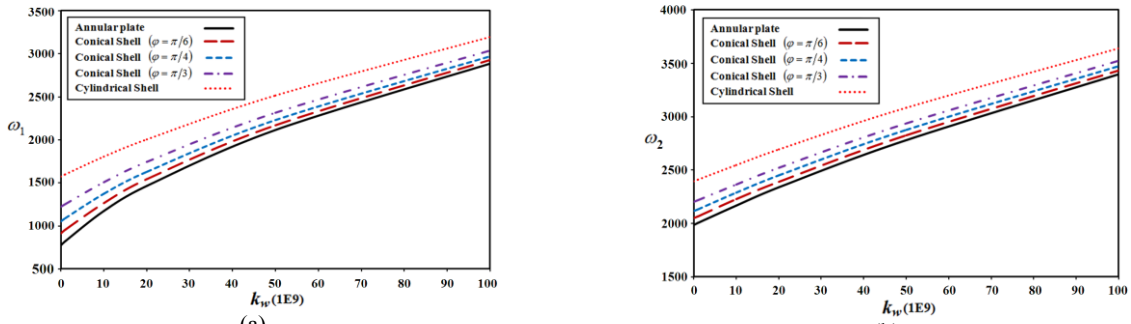

(a) (b)

Fig.2
First two natural frequencies for bidirectional functionally graded shell with clamped-clamped boundary condition (L=R=1, h=0.1, g=1, γ_1= γ_2=0, γ_0=1).

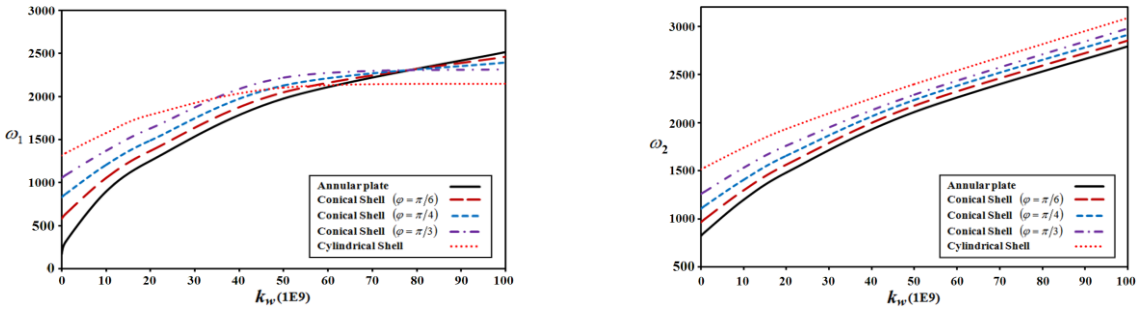

(a) (b)

Fig.3
First two natural frequencies for bidirectional functionally graded shell with free-clamped boundary condition (L=R=1, h=0.1, g=1, γ_1= γ_2=0, γ_0=1).

Table 8
Effect of non-homogeneity of material in two direction on the natural frequencies for different boundary conditions (R = L = 1, γ_i = 0, h = 0.1), Inner edge-outer edge: C-C, S-C.

			$\alpha_0=\alpha_1=1,\ \alpha_2=0$ $\beta_0=\beta_1=1,\ \beta_2=0$			$\alpha_0=\alpha_1=\alpha_2=1$ $\beta_0=\beta_1=1,\ \beta_2=0$			$\alpha_0=\alpha_1=1,\ \alpha_2=5$ $\beta_0=\beta_1=\beta_2=1$		
			$g=1$	$g=2$	$g=5$	$g=1$	$g=2$	$g=5$	$g=1$	$g=2$	$g=5$
Annular Plate (φ=0)	C-C	ω_1	767.16	816.78	878.43	841.88	896.38	964.06	978.37	1041.9	1120.6
		ω_2	1980.7	2113.7	2271.9	2163.1	2308.4	2481.2	2482	2648.9	2847.2
		ω_3	3598.4	3848.4	4134.4	3921.4	4193.9	4505.6	4471.9	4783	5138.5
	S-C	ω_1	588.35	626.1	674	650.38	692.11	745.07	777.82	827.77	891.13
		ω_2	1712.3	1825.4	1963.6	1875.5	1999.3	2150.7	2173.5	2317	2492.6
		ω_3	2812.7	3033.2	3218.6	3146.8	3393.6	3601	3943	4252.1	4511.9
Conical Shell (φ=π/6)	C-C	ω_1	906.84	967.89	1035	991.96	1058.7	1132.2	1149.3	1226.8	1312.2
		ω_2	2042.4	2179.7	2338.3	2228.9	2378.8	2552	2555.6	2727.7	2926.6
		ω_3	3637.9	3889.9	4174.7	3963.5	4238.1	4548.6	4518.5	4832	5186
	S-C	ω_1	769.44	822.03	877.06	840.04	897.38	957.83	982.99	1050	1121.6
		ω_2	1780.7	1898.8	2037.1	1948.2	2077.3	2229	2254.3	2403.8	2579.8
		ω_3	2762.2	2978.4	3160.4	3095	3337.1	3540.9	3889.9	4193.9	4449.6
Conical Shell (φ=π/4)	C-C	ω_1	1051.8	1124.7	1199.1	1148	1227.6	1308.9	1326.9	1419.1	1513.4
		ω_2	2109.5	2252.3	2413.3	2300.5	2456.3	2632	2636	2814.8	3016.4
		ω_3	3678.7	3933.6	4219.1	4007	4284.7	4595.8	4566.7	4883.6	5238.3
	S-C	ω_1	940.73	1007.4	1071.6	1020.6	1092.9	1162.9	1180.5	1264	1346.1
		ω_2	1854.1	1978.5	2119.2	2026.4	2162.2	2316.4	2341.7	2498.5	2677.5
		ω_3	2704	2914.8	3092.2	3035.2	3271.6	3470.5	3828.4	4126.3	4376.7
Conical Shell (φ=π/3)	C-C	ω_1	1221.9	1308.6	1392.3	1330.8	1425.2	1516.5	1533.8	1642.8	1748.5
		ω_2	2194.5	2344.5	2509	2391.4	2554.9	2734.4	2738.5	2925.9	3131.7
		ω_3	3730.4	3989.2	4276.1	4062.3	4344.1	4656.8	4628.2	4949.7	5306.1
	S-C	ω_1	1126.9	1209	1284.2	1216.6	1305.2	1386.8	1394.9	1496.4	1591
		ω_2	1945.9	2078.2	2222.5	2124.2	2268.5	2426.6	2451.5	2617.9	2801.3
		ω_3	2631.2	2834.7	3006.1	2960.7	3189.5	3382.1	3751.6	4041.4	4285
Cylindrical Shell (φ=π/2)	C-C	ω_1	1567	1681.5	1785.3	1695.5	1819.3	1932	1934.9	2076.4	2205.9
		ω_2	2385.4	2551.7	2725.2	2597.8	2778.9	2968.1	2973.8	3181.6	3398.4
		ω_3	3849.2	4117.4	4408.5	4190.6	4482.7	4799.8	4772.6	5106	5467.3
	S-C	ω_1	1428.7	1537.9	1633.4	1532	1648.7	1751.3	1739.5	1871.2	1988.7
		ω_2	2143.2	2293.1	2446.3	2336.4	2499.7	2667.4	2695.9	2884.1	3078.8
		ω_3	2515.7	2703.7	2862.9	2840.7	3053.3	3233.1	3616.7	3888.5	4117.5

The effect of nonlinearity of elastic foundation on the natural frequencies are investigated in Table 9 by means of considering foundation coefficients, γ_i. It is interesting to note that the presence of elastic foundation cause the ω_i to

be increased because the structure will be stiffer. Moreover, when the stiffness of foundation changes from constant variation to linear and parabolic variation, the effect of elastic foundation is much pronounce.

Table 9
Effect of nonlinear elastic foundation on first three natural frequencies of the FGM annular, conical and cylindrical shells (g = 1).

		$k_w = 10^9$						$k_w = 10^9\left(1+x/L\right)$		$k_w = 10^9\left(1+2x/L+5x^2/L^2\right)$	
		C-C			F-C			F-C	C-C	C-C	F-C
		Present	3D (ABAQUS)	Difference (%)	Present	3D (ABAQUS)	Difference (%)	Present		Present	
Annular Plate (φ=0)	ω_1	819.67	824.06	0.53	321.86	322.06	0.06	842.84	345.84	923.07	397.71
	ω_2	2005.2	2020.7	0.77	864.71	867.56	0.33	2014.6	882.73	2052.6	949.63
	ω_3	3614.7	3652.2	1.03	2090.3	2101.9	0.55	3619.8	2098.8	3641.5	2134.4
Conical Shell (φ=π/6)	ω_1	950.56	954.8	0.44	643.02	644.04	0.16	970.74	656.75	1041.9	689.81
	ω_2	2066.1	2081.3	0.73	1000.7	1002.9	0.22	2075.2	1015.6	2112	1072.3
	ω_3	3654.1	3691.5	1.01	2143.6	2154.7	0.52	3659.2	2151.7	3680.6	2185.7
Conical Shell (φ=π/4)	ω_1	1088.9	1093.9	0.46	873.15	876.61	0.39	1106.7	884.38	1170.1	912.57
	ω_2	2132.5	2147.3	0.69	1137.6	1140.3	0.24	2141.3	1149.9	2176.9	1198.2
	ω_3	3695.1	3731.8	0.98	2197.5	2207.7	0.46	3700.1	2205.1	3721.2	2236.5
Conical Shell (φ=π/3)	ω_1	1253.8	1260.4	0.52	1088.8	1095.5	0.61	1269.3	1098.3	1325.4	1122.5
	ω_2	2216.9	2231.4	0.65	1287.1	1291.6	0.35	2225.4	1297.6	2259.5	1339.5
	ω_3	3747.1	3783.1	0.95	2242.6	2248.9	0.28	3752	2247.6	3772.9	2266.1
Cylindrical Shell (φ=π/2)	ω_1	1595.8	1588.7	0.45	1344.6	1356.9	0.91	1607.9	1350	1651.5	1362.6
	ω_2	2408.6	2405.1	0.14	1538.8	1547.6	0.57	2416.4	1548.5	2448.1	1585.5
	ω_3	3868	3879.1	0.29	2174.3	2173.2	0.05	3872.8	2175.2	3893.1	2177.9

5 CONCLUSION

In this paper, free vibration analysis of bidirectional FG conical and cylindrical shells and annular plates resting on non-constant elastic foundation were investigated based on the FSDT. The mechanical properties were assumed to vary exponentially along the transverse direction and parabolic in the meridian/radial direction. The elastic foundation was considered as a Winkler model with parabolic variation. Six complex equations of motion under proposed unified formulation considerations were analytically solved by using differential transform method. In all numerical assessment, comparison studies were conducted with FEM results to prove high accuracy of the current analytical approach. Fundamental frequencies of conical and cylindrical shells and annular plates under different combinations of free-end, simply-supported and clamped edge conditions were comprehensively studied by considering the effects of thickness, radius, non-homogeneity material parameters and foundation stiffness parameters.

REFERENCES

[1] Qatu M.S., 2004, *Vibration of Laminated Shells and Plates*, San Diego, Elsevier.

[2] Reddy J.N., 2003, *Mechanics of Laminated Composite Plates and Shells: Theory and Analysis*, Florida, CRC Press.

[3] Shen H-S., 2009, *Functionally Graded Materials: Nonlinear Analysis of Plates and Shells*, Taylor & Francis Group, LLC.

[4] Carrera E., Brischetto S., Nali P., 2011, *Plates and Shells for Smart Structures: Classical and Advanced Theories for Modeling and Analysis*, John Wiley & Sons.

[5] Tornabene F., Fantuzzi N., 2014, *Mechanics of Laminated Composite Doubly Curved Shell Structures*, Società Editrice Esculapio, Milan.

[6] Efraim E., Eisenberger M., 2007, Exact vibration analysis of variable thickness thick annular isotropic and FGM plates, *Journal of Sound and Vibration* **29**: 720-738.

[7] Hosseini-Hashemi Sh., Fadaee M., Es'haghi M., 2010, A novel approach for in-plane/out-of-plane frequency analysis of functionally graded circular/annular plates, *International Journal of Mechanical Sciences* **52**: 1025-1035.

[8] Nie G.J., Zhong Z., 2010, Dynamic analysis of multi-directional functionally graded annular plates, *Applied Mathematical Modelling* **34**: 608-616.

[9] Malekzadeh P., Golbahar Haghighi M.R., Atashi M.M., 2011, Free vibration analysis of elastically supported functionally graded annular plates subjected to thermal environment, *Meccanica* **46**: 893-913.
[10] Jodaei A., Jalal M., Yas M.H., 2012, Free vibration analysis of functionally graded annular plates by state-space based differential quadrature method and comparative modeling by ANN, *Composites Part B: Engineering* **43**: 340-353.
[11] Dong C.Y., 2008, Three-dimensional free vibration of functionally graded annular plates using the Chebyshev-Ritz method, *Materials & Design* **29**: 1518-1525.
[12] Shariyat M., Alipour M.M., 2011, Differential transform vibration and modal stress analyses of circular plates made of two-directional functionally graded materials resting on elastic foundations, *Archive of Applied Mechanics* **81**(9): 1289-1306.
[13] Alipour M.M., Shariyat M., 2011, A power series solution for free vibration of variable thickness Mindlin circular plates with two-directional material heterogeneity and elastic foundations, *Journal of Solid Mechanics* **3**(2): 183-197.
[14] Alipour M.M., Shariyat M., 2010, Stress analysis of two-directional FGM moderately thick constrained circular plates with non-uniform load and substrate stiffness distributions, *Journal of Solid Mechanics* **2**(4): 316-331.
[15] Shariyat M., Alipour M.M., 2013, A power series solution for vibration and complex modal stress analyses of variable thickness viscoelastic two-directional FGM circular plates on elastic foundations, *Applied Mathematical Modelling* **37**(5): 3063-3076.
[16] Shariyat M., Alipour M.M., 2014, A novel shear correction factor for stress and modal analyses of annular FGM plates with non-uniform inclined tractions and non-uniform elastic foundations, *International Journal of Mechanical Sciences* **87**: 60-71.
[17] Lezgy-Nazargah M., 2015, Fully coupled thermo-mechanical analysis of bi-directional FGM beams using NURBS isogeometric finite element approach, *Aerospace Science and Technology* **45**: 154-164.
[18] Shariyat M., Jafari A.A., Alipour M.M., 2013, Investigation of the thickness variability and material heterogeneity effects on free vibration of the viscoelastic circular plates, *Acta Mechanica Solida Sinica* **26**(1): 83-98.
[19] Alipour M.M., Shariyat M., Shaban M., 2010, A semi-analytical solution for free vibration and modal stress analyses of circular plates resting on two-parameter elastic foundations, *Journal of Solid Mechanics* **2**(1): 63-78.
[20] Lezgy-Nazargah M., Cheraghi N., 2017, An exact Peano Series solution for bending analysis of imperfect layered FG neutral magneto-electro-elastic plates resting on elastic foundations, *Mechanics of Advanced Materials and Structures* **24**(3): 183-199.
[21] Lezgy-Nazargah M., Meshkani Z., 2018, An efficient partial mixed finite element model for static and free vibration analyses of FGM plates rested on two-parameter elastic foundations, *Structural Engineering and Mechanics* **66**(5): 665-676.
[22] Najafizadeh M.M., Isvandzibaei M.R., 2007, Vibration of functionally graded cylindrical shell based on higher order shear deformation plate theory with ring support, *Acta Mechanica* **191**: 75-91.
[23] Matsunaga H., 2008, Free vibration and stability of functionally graded circular cylindrical shells according to a 2D higher-order deformation theory, *Composite Structures* **88**: 519-531.
[24] Santos H., MotaSoares C.M., MotaSoares C.A., Reddy J.N., 2009, A semi-analytical finite element model for the analysis of cylindrical shells made of functionally graded materials. *Composite Structures* **91**: 427-432.
[25] Zhao X., Lee Y.Y., Liew K.M., 2009, Thermoelastic and vibration analysis of functionally graded cylindrical shells, *International Journal of Mechanical Sciences* **51**: 694-707.
[26] Vel S.S., 2010, Exact elasticity solution for the vibration of functionally graded anisotropic cylindrical shells, *Composite Structures* **92**: 2712-2727.
[27] Shen H.S., 2012, Nonlinear vibration of shear deformable FGM cylindrical shells surrounded by an elastic medium, *Composite Structures* **94**: 1144-1154.
[28] Ebrahimi M.J., Najafizadeh M.M., 2014, Free vibration analysis of two-dimensional functionally graded cylindrical shells, *Applied Mathematical Modelling* **38**: 308-324.
[29] Ng T.Y., He X.Q., Liew K.M., 2002, Finite element modeling of active control of functionally graded shells in frequency domain via piezoelectric sensors and actuators, *Computational Mechanics* **28**: 1-9.
[30] Pradhan S.C., Loy C.T., Lam K.Y., Reddy J.N., 2000, Vibration characteristics of functionally graded cylindrical shells under various boundary conditions, *Applied Acoustics* **61**:111-129.
[31] Viola E., Rossetti L., Fantuzzi N., 2012, Numerical investigation of functionally graded cylindrical shells panels using the generalized unconstrained third order theory coupled with the stress recovery, *Composite Structures* **94**: 3736-3758.
[32] Bhangale R.K., Ganesan N., Chandramouli P., 2006, Linear thermoelastic buckling and free vibration behavior of functionally graded truncated conical shells, *Journal of Sound and Vibration* **292**: 341-371.
[33] Tornabene F., 2009, Free vibration analysis of functionally graded conical, cylindrical shell and annular plate structures with a four-parameter power-law distribution, *Computer Methods in Applied Mechanics and Engineering* **198**: 2911-2935.
[34] Tornabene F., Viola E., Inman D.J., 2009, 2-D differential quadrature solution for vibration analysis of functionally graded conical, cylindrical shell and annular plate structures, *Journal of Sound and Vibration* **328**: 259-290.
[35] Qu Y.G., Long X.H., Yuan G.Q., Meng G., 2013, A unified formulation for vibration analysis of functionally graded shells of revolution with arbitrary boundary conditions, *Composites Part B: Engineering* **50**: 381-402.
[36] Sofiyev A.H., 2009, The vibration and stability behavior of freely supported FGM conical shells subjected to external pressure, *Composite Structures* **89**: 356-366.

[37] Sofiyev A.H., 2011, On the vibration and stability of clamped FGM conical shells under external loads, *Journal of Composite Materials* **45**: 771-788.
[38] Malekzadeh P., Fiouz A.R., Sobhrouyan M., 2012, Three-dimensional free vibration of functionally graded truncated conical shells subjected to thermal environment, *International Journal of Pressure Vessels and Piping* **89**: 210-221.
[39] Sofiyev A.H., 2012, The non-linear vibration of FGM truncated conical shells, *Composite Structures* **94**: 2237-2245.
[40] Najafov A.M., Sofiyev A.H., 2013, The non-linear dynamics of FGM truncated conical shells surrounded by an elastic medium, *International Journal of Mechanical Sciences* **66**: 33-44.
[41] Malekzadeh P., Heydarpour Y., 2013, Free vibration analysis of rotating functionally graded truncated conical shells, *Composite Structures* **97**: 176-188.
[42] Sofiyev A.H., 2014, On the dynamic buckling of truncated conical shells with functionally graded coatings subject to a time dependent axial load in the large deformation, *Composites: Part B* **58**: 524-533.
[43] Sofiyev A.H., 2014, The combined influences of heterogeneity and elastic foundations on the nonlinear vibration of orthotropic truncated conical shells, *Composites: Part B* **61**: 324-339.
[44] Xiang X., Guoyong J., Tiangui Y., Zhigang L., 2014, Free vibration analysis of functionally graded conical shells and annular plates using the Haar wavelet method, *Applied Acoustics* **85**: 130-142.
[45] Zhu S., Guoyong J., Shuangxia Sh., Tiangui Y., Xingzhao J., 2014, A unified solution for vibration analysis of functionally graded cylindrical, conical shells and annular plates with general boundary conditions, *International Journal of Mechanical Sciences* **80**: 62-80.
[46] Zhu S., Guoyong J., Tiangui Y., 2014, Three-dimensional vibration analysis of thick functionally graded conical, cylindrical shell and annular plate structures with arbitrary elastic restraints, *Composite Structures* **118**: 432-447.
[47] Tornabene F., Fantuzzi N., Bacciocchi M., 2014, Free vibrations of free-form doubly-curved shells made of functionally graded materials using higher-order equivalent single layer theories, *Composites: Part B* **67**: 490-509.
[48] Sofiyev A.H., Kuruoglu N., 2015, On a problem of the vibration of functionally graded conical shells with mixed boundary conditions, *Composites: Part B* **70**: 122-130.